

# An Algorithm for Heart Rate Extraction in a Novel Wearable Acoustic Sensor

Guangwei Chen, Syed Anas Imtiaz, Eduardo Aguilar-Pelaez and Esther Rodriguez-Villegas

Department of Electrical and Electronic Engineering, Imperial College London, SW7 2AZ, UK

Submission for Wearable Healthcare Technology Special Issue in Healthcare Technology Letters.

Phonocardiography is a widely used method of listening to the heart sounds and indicate the presence of cardiac abnormalities. Each heart cycle consists of two major sounds - S1 and S2 - which can be used to determine the heart rate. The conventional method of acoustic signal acquisition involves placing the sound sensor at the chest where this sound is most audible. In this paper, we present a novel algorithm for the detection of S1 and S2 heart sounds and using them to extract the heart rate from signals acquired by a small sensor placed at the neck. This algorithm achieves an accuracy of 90.73% and 90.69%, with respect to heart rate value provided by two commercial devices, evaluated on more than 38 hours of data acquired from ten different subjects during sleep in a pilot clinical study. This is the largest dataset for acoustic heart sound classification and heart rate extraction in the literature to date. The algorithm in this paper used signals from a sensor designed to monitor breathing. This shows that the same sensor and signal can be used to monitor both breathing and heart rate making it highly useful for long term wearable vital signs monitoring.

**1. Introduction:** Heart sounds have been a source of information for diagnosis of patients' conditions since the late nineteenth century via the use of the stethoscope [1]. Trained doctors can listen for abnormal heart sounds in what is commonly referred to as cardiac auscultation. The conventional method of analysing heart sounds is known as phonocardiography (PCG) where a microphone, normally placed on the chest, is used to record the sounds which can be analysed by a doctor. Each heart cycle consists of two major sounds: S1 followed by S2. Other sounds and murmurs can indicate abnormalities. The distance between two S1 sounds is the duration of one heart cycle that can be used to determine the heart rate.

PCG has been used broadly for diagnosis of certain cardiac conditions and has in the later part of the 20<sup>th</sup> century received attention by the engineering community with the goal of investigating signal processing techniques to achieve automatic segmentation and marking of PCG signals. The capability of segmenting heart sound into heart cycles and distinguishing between cardiac phases, by appropriately detecting the first and second heart sound, is useful since it can be used to calculate the heart rate.

Several research groups have used different signal processing techniques for the segmentation of the two main heart sounds - S1 and S2 - from PCG signals for different applications including the evaluation of heart rate. These can be broadly divided into two categories [2]. First, those that use ECG as a reference for synchronization of heart cycles and, second, those that rely solely on the PCG signal without any reference. The latter approach is appropriate for wearable devices since it relies on smaller number of sensors. This section briefly reviews some of these techniques that do not require ECG reference and reports their accuracy.

Liang et al. [3] presented a method for heart sound segmentation by detecting peaks from the normalised average Shannon energy of the low pass filtered input signal. They tested the algorithm using 515 cardiac cycles obtained from 37 subjects and reported sensitivities of 93% and 84% on clean and normal signals respectively. They further improved their algorithm's performance by using wavelet decomposition [4] instead of low pass filtering, with sensitivities of 96.7% and 93% on clean and normal signals. Brusco and Nazeran [5] presented an algorithm, also using peaks from the normalised Shannon energy, for the classification of different heart sounds. For the segmentation of S1 and S2 sounds they used a threshold to classify the peaks and considered the distances between them. They achieved an overall accuracy of 79.3% for the detection of heart cycles. In another method, Kumar et al. [2] used wavelet decomposition of the input signal to extract

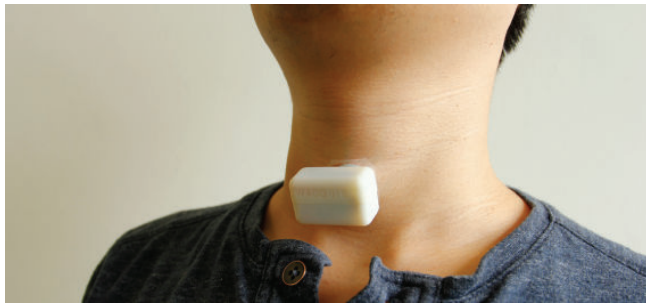
high frequency components. They used Shannon energy of these components for classification of S1 and S2 sounds and estimation of heart rate. Their dataset consisted of a maximum of 110 minutes of data recorded from 55 patients with 7530 heart cycles and achieved a sensitivity of 97.95%. Wang et al. [6] also used Shannon energy of the signal in a multistage method for the segmentation of S1 sounds. They first used wavelet transform to isolate potential S1 and S2 sounds followed by detection of S1 using Shannon energy. They reported sensitivity of 93.2% with test data consisting of 207 heart cycles.

Gamero and Watrous [7] employed a statistical approach using Hidden Markov Model (HMM) for the classification of S1 and S2 sounds. Their data set included 20 second recording each from 80 subjects and their algorithm achieved a sensitivity of 95%. Ricke et al. [8] also used HMM after computing the Shannon energy of the input signal. They reported a sensitivity of 98% on a test set that consisted of 2286 seconds of clean (noise free) data. Using wavelet decomposition and HMM, Lima and Barbosa [9] reported 99.1% sensitivity for the detection of S2 sounds from 700 heart cycles.

Ari et al. [10] presented a method in which the PCG signal is first low-pass filtered with a cutoff frequency of 150 Hz. The energy peaks from the filtered signal are extracted using a varying threshold that are then classified in an iterative process involving time search and amplitude threshold reduction. They reported the algorithm's accuracy as 97.5% using a test set with 357 heart cycles. Yamacli et al. [11] performed wavelet decomposition of the normalised input signal followed by moving window integration of the squared (energy) signal. The energy peaks are then detected by a varying threshold which are classified as S1 or S2 based on time conditions. With 326 heart cycles from 53 patients they reported sensitivities of 91.47% and 88.95% for S1 and S2 classification respectively. Gupta et al. [12] used wavelet features with a grow and learn (GAL) algorithm to successfully segment 90.29% of 340 heart cycles with murmurs. Finally, Chen et al. [13] presented a PCG-based heart rate measurement method using template extraction and matching of the filtered input signal. They used three subjects for testing and reported a root mean square (RMS) error value in the calculation of heart rate as 2.4 bpm with the subjects in resting position.

In all of the methods above, the sensor to record heart sounds was placed on the chest. Most of these sensors were either bulky or required strapping around the chest which adds to the discomfort of the user.

Popov et al. [14] used a different approach involving a piezoelectric sensor placed on the throat to acquire carotid pulse sounds. They applied autocorrelation analysis to 20-second recording sections of bandpass filtered input signal for the



(a)



(b)

**Figure 1** (a) Acoustic sensor being worn by a subject on the neck. (b) Second generation of the sensor with a smaller size (compared against a two pence coin).

estimation of heart rate. They used 10 minute recordings from 8 subjects during treadmill exercise and achieved a standard deviation of 3.4 bpm. However, the bias of the regression estimation is large. For a heart rate of 60 bpm, the bias would be +11.75 bpm.

In our prior work we used a wearable sensor placed at the suprasternal notch to monitor breathing [15]. The sensor, shown in Fig. 1, acquired signals that also included heart sounds. For the detection of respiratory rate, heart sounds are considered as interference and need to be removed. However, once localized these can be used to detect the S1 and S2, and subsequently the heart rate.

The signals acquired at the suprasternal notch are intrinsically different to those observed at the surface of the chest. Signals measured at the chest have travelled a short distance propagating from the heart, through lung tissue and finally through muscle and bone. This allows for the signal to be less filtered and have higher frequency components. Signals measured at the suprasternal notch have travelled a greater distance from the heart and principally propagated along the arterial wall of the carotid artery. As a result, the signals are of similar timing characteristics but of significantly lower bandwidth. However, the use of one small sensor to perform the dual role of respiratory and heart rate detection is advantageous since it obviates the need for an additional sensor thus making it more comfortable for the subjects undergoing long term monitoring.

In this paper we present a novel algorithm for the detection of heart rate from heart sounds acquired from a sensor placed at the suprasternal notch, originally designed to monitor breathing. Because, the sensor was used to monitor breathing, the heart sound signals are much attenuated and are *corrupted* with respiratory signals. The idea of the algorithm described in this paper is to recover the heart sound signals from the respiratory signal and then evaluate the heart rate. Section 2 explains the different stages of this algorithm in detail. Section 3 describes the dataset of over 38 hours of acoustic signals used to test the algorithm. The performance of the algorithm for the calculation of heart rate is presented in Section 3 and further discussed with conclusions in Section 4.

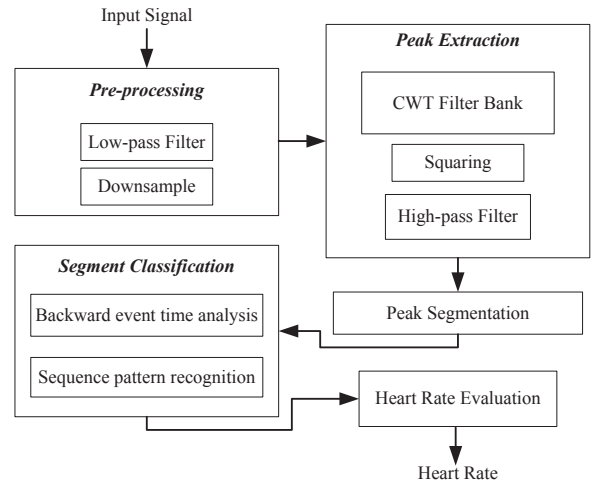


**Figure 2** Block diagram of the proposed algorithm showing all the processing stages.

**2. Algorithm:** In this section a novel algorithm for the detection of heart rate is presented. The input acoustic signal is first filtered to be in the frequency of interest. It is analyzed with a CWT based filter bank to extract peak frequencies that can be potential S1 and S2 sounds. The peaks are later grouped together and classified with a dynamic detection threshold using a set of rules to identify S1 and S2 events. A block diagram of the proposed algorithm is shown in Fig. 2 and the details of each processing stage are given below.

**2.1. Pre-processing:** The input signal, sampled at 2205 Hz using a 10-bit ADC, is initially filtered with an 8<sup>th</sup> order low pass filter with a cutoff frequency of 100 Hz. The cutoff frequency is chosen based on the signal characteristics. The filtered signal is subsequently downsampled by a factor of 10 to reduce data rate for reduction of unnecessary computational complexity due to the very high oversampling of heart sounds (originally meant for breathing sounds). As a result, the new sampling frequency is 220.5 Hz. An example of the input signal before and after filtering and downsampling is shown in Fig. 3.

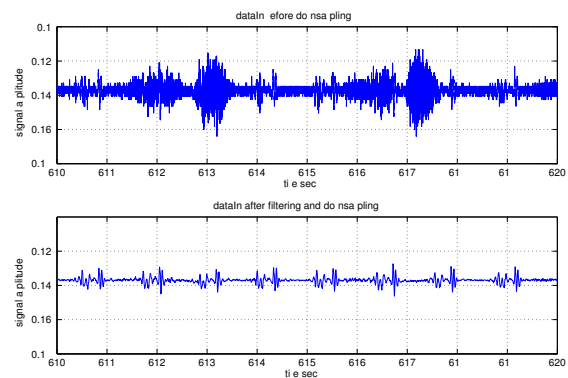


**Figure 3** An example of input signal section before and after filtering with a 8<sup>th</sup> order LPF at 100Hz and downsampling from 2205Hz to 220.5Hz.

**2.2. Peak Extraction:** In order for the heart sounds to be detected the peaks of energy in the time-frequency plane need to be located. Because of the variation in peak frequencies between S1 and S2 sounds as well as between different subjects a filter

bank approach provides better resolution than a broader single bandpass filter approach encompassing the region where energy peaks are expected. The specifications required of this filter bank are particular in that both time resolution and frequency resolution are important. In other words the bandwidth of each filter needs to be as narrow as possible whilst still guaranteeing a short enough impulse response.

The filter bank is realized using Continuous Wavelet Transform (CWT) filters with Meyer mother wavelet. The centre frequencies of the filter bank were chosen to be a spread of 15 filters ranging from 8.9 Hz all the way until 23 Hz focusing on the frequency region where peaks are expected to occur. The output of the CWT filter can have both positive and negative values given that the intrinsic transformation performed is a convolution in time of the signal and the mother wavelet. Thus, the output is squared so that the peaks on both positive and negative side of the signal can be utilised.

The filter bank covers a selective frequency range which extends further than the normal bandwidth of single heart sounds S1 and S2. Further, heart sounds can have varied peak frequencies between different subjects. Thus, the highest squared value output of the CWT filter bank for each sample was selected to allow for such inter-subject variations. In some cases high amplitude artefacts can maximize the value of the CWT filter bank output. However, these artefacts, resulting from loud breathing, snoring or speaking have a longer duration than heart sounds (longer than 200 ms) and can be discriminated later in the algorithm.

A high-pass filtering is performed on the output of the filter bank for better selection of transient-like signals once the peaks have been extracted. This is achieved using an 8<sup>th</sup> order finite impulse response (FIR) filter with a cutoff frequency of 40 Hz.

**2.3. Signal Grouping/Segmentation and Classification:** The extracted peaks are then verified using an amplitude threshold that varies dynamically along time as a function of the input signal. Multiple peaks that are above the threshold and separated by less than 100 ms are grouped together in one segment. The duration of the segment is then defined by it starting at the first part of the signal above threshold and finishing at the last, encompassing all the samples in between.

The detection threshold starts off at a given value but gets updated to a proportional value of the peak amplitude (equation 1) when a segment is classified as heart sound following the normal expected time conditions in the later blocks of the signal processing. The coefficients  $c_1$  and  $c_2$  are defined to be 0.9 and 0.1 respectively whilst the ratio factor  $r_1$  is set to  $\frac{1}{3}$ . If there is a long section where all values are above or below the threshold then it is reset to initial value. This long section is the time in which five S1 sounds are expected.

$$thr_{new} = c_1 \times thr_{old} + c_2 \times r_1 \times peakamp(n); \quad (1)$$

Once the segments are identified they are classified as either S1 or S2 using a series of time-based rules.

**2.4. Segment Classification:** This stage consists of a set of conditions that are executed sequentially if the previous one fails. These rules have been divided into two different categories. The first category, *Backward event time analysis*, covers a set of three normal scenarios and four exceptions for classification of a given segment. The second category, *Sequence pattern recognition*, is triggered when the last five segments fall within a certain time pattern. All of these rules are explained in detail below.

**2.4.1. Backward event time analysis:** This method consists of detecting S1 and S2 heart sounds based on the time separation between detected peak segments. It is based on the time separation between peak segments in comparison to two time variables: the

time separating an S1 heart sound and its corresponding S2 ( $D1$ ); and the time difference between two S1 sounds ( $D2$ ) which is equivalent to one heart cycle period.

The algorithm starts with  $D1$  and  $D2$  defined as in equation 2 and updates them dynamically as the algorithm interprets more data (based on conditions below). The  $D1$  to  $D2$  ratio is calculated based on the relationship presented by Weissler *et al.* [16].

For the purpose of detecting peaks when variations in  $D1$  and  $D2$  occur the margin ratios  $k1$  and  $k2$  as described in equation 3 are introduced. These allow for peaks occurring slightly earlier or later (-15% and +10%) with respect to the latest S1 heart sound to be considered in the backward event time analysis. In the following rules the segment classification at  $n$  is denoted by  $sc(n)$  while the segment time is denoted by  $st(n)$ .

$$D1 = 0.32 \text{ sec} \quad D2 = 0.87 \text{ sec} \quad (2)$$

$$k1 = 0.85 \quad k2 = 1.1 \quad (3)$$

**Scenario 1:** This condition checks for the presence of a previously defined S1 at the antepenultimate segment  $sc(n-2)$  to define the current segment  $sc(n)$  as S1. If an S1 exists at  $n-2$ , the condition is passed if the distance between the segments is within the expected margins. Otherwise the segment is labelled as undefined or “don’t know” (DK).

$$sc(n) = S1, \text{ if } \begin{cases} sc(n-2) = S1 \\ st(n) - st(n-2) > k1 \times D2 \\ st(n) - st(n-2) < k2 \times D2 \end{cases} \quad (4)$$

If this condition is passed the time distance  $D2$  is updated as a weighted average between the newly measured time and its previous value as shown below.

$$D2 = 0.9 \times D2 + 0.1 \times (st(n) - st(n-2)) \quad (5)$$

**Scenario 2:** This condition looks for the presence of an S1 at the previous segment  $sc(n-1)$  in order to define the peak at  $n$  as S2 if the time distance to the previous segment is within the  $D1$  time separation expected (S1 to S2 time).

$$sc(n) = S2, \text{ if } \begin{cases} sc(n) = DK \\ sc(n-1) = S1 \\ st(n) - st(n-1) > k1 \times D1 \\ st(n) - st(n-1) < k2 \times D1 \end{cases} \quad (6)$$

If this condition is evaluated to be true the time distance  $D1$  is redefined as a weighted average between the newly measured time and the previous value.

$$D1 = 0.9 \times D1 + 0.1 \times (st(n) - st(n-1)); \quad (7)$$

**Scenario 3:** This condition is similar to the previous case and looks for the presence of an S2 at  $n-1$  to define the segment at  $n$  as S1 if the distance between the present and the penultimate segment is that expected between an S2 and an S1.

$$sc(n) = S1, \text{ if } \begin{cases} sc(n) = DK \\ sc(n-1) = S2 \\ st(n) - st(n-1) > k1 \times (D2 - D1) \\ st(n) - st(n-1) < k2 \times (D2 - D1) \end{cases} \quad (8)$$

In this condition there is no redefinition of  $D1$  or  $D2$  because the analyzed time corresponds to  $D1$ - $D2$  which is a measure between two different heart cycles, not directly correlated to either the periodicity of neuromuscular excitation of the heart ( $D1$ ) or the heart cycle event sequence between and separation between two of its sounds ( $D2$ ).

If the three *normal scenarios* fail to classify a segment it is labelled as *DK*. If two consecutive segments are labelled as *DK* then a further series of *exceptions* are triggered to attempt and define the current segment.

**Exception 1 and 2:** These are two similar conditions (for S1 and S2 respectively) look for a DK at  $n - 1$  to define the peak at  $n$  as S1 or S2 based on what was defined at  $n - 2$  if the separation between the  $n - 2$  and  $n$  peaks is within the D2 margins, i.e. the one between an S1 and an S1 or a S2 and an S2.

$$sc(n) = S1 \text{ or } S2, \text{ if } \begin{cases} sc(n) = DK \\ sc(n-1) = DK \\ sc(n-2) = S1 \text{ or } S2 \text{ respectively} \\ st(n) - st(n-2) > k1 \times D2 \\ st(n) - st(n-2) < k2 \times D2 \end{cases} \quad (9)$$

If the segment at  $n - 2$  was an S1 then D2 is updated using equation 5 as in condition *Scenario 1*.

**Exception 3:** This condition is used to define the current segment as S1 if the time distance to segment  $n - 2$  is  $D2 \times 2 - D1$  and the segment at  $n - 2$  had previously been classified as S2. In this case the segment at  $n - 1$  is left as DK.

$$sc(n) = S1, \text{ if } \begin{cases} sc(n) = DK \\ sc(n-1) = DK \\ sc(n-2) = S2 \\ st(n) - st(n-2) > (k1 \times D2) \times 2 - D1 \\ st(n) - st(n-2) < (k2 \times D2) \times 2 - D1 \end{cases} \quad (10)$$

**Exception 4:** This condition defines the current segment as S1 if the time distance to segment  $n - 2$  is  $D2 - D1$  and the segment at  $n - 2$  had previously been classified as S2. In this case, as in *Exception 3*, the segment at  $n - 1$  is left as DK.

$$sc(n) = S1, \text{ if } \begin{cases} sc(n) = DK \\ sc(n-1) = DK \\ sc(n-2) = S2 \\ st(n) - st(n-2) > (k1 \times D2) - D1 \\ st(n) - st(n-2) < (k2 \times D2) - D1 \end{cases} \quad (11)$$

In the event that all *exceptions* fail to determine whether a segment is S1 or S2, it is left as *DK*.

2.4.2. Sequence pattern recognition: The pattern recognition strategy has been designed to provide the least possible false S1 and S2 detections. The last five peak segments must fall within particular time location restrictions in order for a pattern to be detected and considered as correct S1 and S2 heart sounds. This is useful at the start of the classification when the algorithm is initialized and after any discontinuity in peaks that could not be dealt with by any of the *Scenarios* and *Exception* conditions.

$$sc(n-4:n) = \begin{cases} [S2, S1, S2, \\ S1, S2], \text{ if } \begin{cases} st(n) - st(n-1) > k1 \times D1 \\ st(n) - st(n-1) < k2 \times D1 \\ st(n) - st(n-2) > k1 \times D2 \\ st(n) - st(n-2) < k2 \times D2 \\ st(n) - st(n-3) > k1 \times D1 + D2 \\ st(n) - st(n-3) < k2 \times D1 + D2 \\ st(n) - st(n-4) > k1 \times D2 + D2 \\ st(n) - st(n-4) < k2 \times D2 + D2 \end{cases} \end{cases} \quad (12)$$

**Patterns 1 and 2:** These two patterns defined in equations (12) and (13) respectively look for cases where the preceding four segments have not been classified but happen to follow a time separation pattern with the present segment that coincides with that expected based on the time separations D1 and D2 at that particular point in time. It is important to remember that the time separations D1 and D2 are dynamic values that are updated as candidate S1 and S2 events are detected.

$$sc(n-4:n) = \begin{cases} [S1, S2, S1, \\ S2, S1], \text{ if } \begin{cases} st(n) - st(n-1) > k1 \times D2 - D1 \\ st(n) - st(n-1) < k2 \times D2 - D1 \\ st(n) - st(n-2) > k1 \times D2 \\ st(n) - st(n-2) < k2 \times D2 \\ st(n) - st(n-3) > k1(D2 - D1) + D2 \\ st(n) - st(n-3) < k2(D2 - D1) + D2 \\ st(n) - st(n-4) > k1 \times D2 + D2 \\ st(n) - st(n-4) < k2 \times D2 + D2 \end{cases} \end{cases} \quad (13)$$

**Pattern 3:** This condition consists of detecting a pattern where there is some peak time separation repetition similar to that expected from S1 and S2 sounds but where this time separation recognition is not limited by the D1 and D2 bounds presented above. To detect a new pattern without these bounds, a new D2 is defined as the time separation between the present segment at  $n$  and the second preceding one ( $n - 2$ ). This way regardless of whether the present segment is S1 or S2, the time difference between the two is taken as being one heart cycle duration (equation (14)).

$$D2_x = st(n) - st(n-2) \quad (14)$$

For pattern 3 to be evaluated the newly defined D2 separation ( $D2_x$ ) needs to pass one further condition. This is based on the expected limit of heart rate variation and maximum heart rate for pattern recognition ( $HR_{max} = 200\text{bpm}$ ). Equation 15 defines the upper limit of heart rate variability (increase) which has been defined considerably high so as to only remove the cases that are clearly above the expected ranges of HR increase and to allow for enough dynamic variation.

$$HR_{var \text{ limit}} = 3.77 \times (\text{seconds since last } D2 \text{ update}) + 17 \quad (15)$$

$$HR_{measured \text{ var}} = \frac{60}{D2_x} - \frac{60}{D2_{last}} \quad (16)$$

The condition for carrying out the pattern 3 evaluation is defined in equation 17.

$$\text{Conditions for testing pattern 3} = \begin{cases} HR_{measured \text{ var}} < HR_{var \text{ limit}} \\ \frac{60}{D2_x} < HR_{max} \end{cases} \quad (17)$$

Once these conditions are met, a new value of D1 is defined based on the correlation presented in [16], shown in equation 18.

$$D1_x = -0.0018 \times \frac{60}{D2_x} + 0.456 \quad (18)$$

$$sc(n-4:n) = \begin{cases} st(n) - st(n-1) > k1 \times D1_x \\ [S2, S1, S2, < k2 \times D1_x \\ S1, S2], if \left\{ \begin{array}{l} st(n) - st(n-3) > k1 \times D1_x + D2_x \\ < k2 \times D1_x + D2_x \\ st(n) - st(n-4) > k1 \times D2_x + D2_x \\ < k2 \times D2_x + D2_x \end{array} \right. \end{cases} \quad (19)$$

**Pattern 4:** This condition is effectively the same as *Pattern 3* but with the exception that  $D1_x$  is defined as the last value of D1.

**Pattern 5:** This condition looks for time separations that would have been caused by S1 sounds and hence separated by their respective D2. It also needs to pass the same conditions of heart rate variability and maximum heart rate as expressed in equation 17. The new D2 is defined based on the separation of the last two segments (equation 20).

$$D2_x = st(n) - st(n-1) \quad (20)$$

$$sc(n-4:n) = \begin{cases} st(n-1) - st(n-2) > k1 \times D2_x \\ [S1, S1, S1, < k2 \times D2_x \\ S1, S1], if \left\{ \begin{array}{l} st(n-2) - st(n-3) > k1 \times D2_x \\ < k2 \times D2_x \\ st(n-3) - st(n-4) > k1 \times D2_x \\ < k2 \times D2_x \end{array} \right. \end{cases} \quad (21)$$

2.5. Heart rate calculation: In order for the heart rate to be calculated based on the classification of segments as S1 or S2, heart beat cycles need to be detected. Therefore, any S2 following an S1 is merged to the corresponding S1 so as to form a single entity representing a single heart beat. The number of heart beats detected in a particular *time* interval is then used to calculate the heart rate using equation 22.

$$Heart\ Rate = \frac{num\ of\ intervals}{time\ (sec)} \times 60 \quad (22)$$

### 3. Performance Analysis:

3.1. Database: Data was obtained as part of a clinical study which was conducted in a sleep study room of the National Hospital for Neurology and Neurosurgery (UK). The study was approved by the Medicine and Healthcare products Regulatory Agency (MHRA) and the Research Ethics Committee of the UK National Hospital for Neurology and Neurosurgery. A wireless acoustic sensor was placed at the suprasternal notch during night time which sampled data at a frequency of 2205 Hz and transmitted to a nearby base station for further analysis.

At the same time, two external devices were used to compute reference heart rate for performance evaluation: SOMNOscreen by SomnoMedics [17] and PULSOX 300i pulse oximeter by Konica Minolta [18]. The SomnoMedics device provides a pulse output calculated based on the photoplethysmography signal which is used by a software to calculate the heart rate. The Konica Minolta pulse oximeter also provides its own heart rate numerical output along with the oxygen saturation based on its own photoplethysmography sensor. Data from all three sensors was synchronized at the end of each recording using a single reference clock and a total of over 38 hours of data recorded during sleep from ten different subjects was evaluated. The heart rate varied differently for each subject throughout the night. The range of variation and the median heart rate for all subjects is shown in Fig. 4.

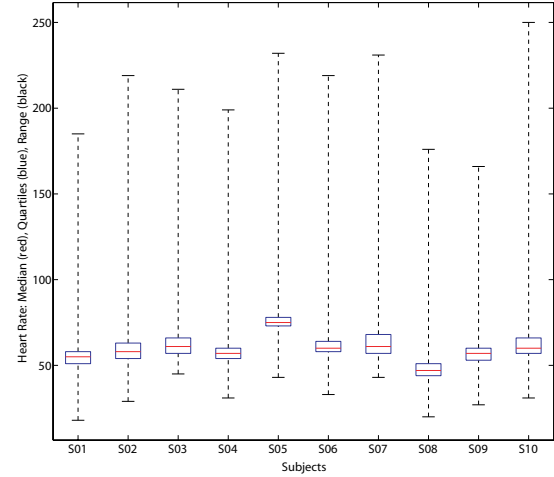


**Figure 4** Heart rate variation and ranges in each subject as recorded by the reference device.

3.2. Results: The proposed algorithm computes heart rate in a window of 60 seconds. This was compared with the values obtained from two commercial monitors: SomnoMedics and Konica-Minolta. They have a sampling rate of 4 Hz and 1 Hz respectively, therefore the average value over 60 seconds from these sensors was used to compare the output from the algorithm.

The numerical difference of the values calculated by the algorithm and those provided by the two external devices have been characterised by the quartile divisions of the difference spread. The results show that in most cases the algorithm achieves a high concentration of outcomes very close to zero difference with short separation between quartiles. The median difference for all subjects in both cases is less than 0.5 bpm except for S07 where the greater than normal spread is attributed to sustained presence of snoring throughout the night – even if not always saturating the ADC – and the resulting necessity for the algorithm to continuously look for patterns. The reason for this is that after a large snore which interrupts the classification of heart sounds via the more robust *scenarios* and *exception* conditions the algorithm needs to restart the classification by finding a pattern which is more prone to errors under bad signal conditions.

To determine the overall accuracy of the algorithm the percentage of heart rate output values that fit within a narrow error margin of  $\pm 10\%$  with respect to the values provided by the gold standard reference devices was calculated. The results of the algorithm expressed in this performance metric for each subject and in comparison to each reference device are shown in Table 1. From this it can be noticed that the algorithm achieved results above 90% for 6 of the 10 subjects (above 85% for 9 subjects) and that the lowest value was from subject S07 for reasons explained above. The overall weighted accuracy of the algorithm is 90.73% and 90.69% with respect to the Konica-Minolta and SomnoMedics devices respectively based on the duration of data per subject.

**4. Discussion:** An algorithm for the segmentation of heart sounds (S1 and S2) and extraction of heart rate from signals recorded at suprasternal notch is presented in this paper. The performance of this algorithm has been evaluated on over 38 hours of data acquired from 10 different subjects during sleep in the clinical trial setting. To the best of authors' knowledge, this represents the largest data set a heart sound classification and heart rate extraction algorithm has been tested on. Although other studies (such as [3], [4], [11]) used data from a greater number of subjects, their total duration of data and the number of heart cycles was significantly smaller.

**Table 1** Percentage accuracy of algorithm with respect to Konica-Minolta and SomnoMedics devices for each subject and their weighted average.

Subject	Konica-Minolta	SomnoMedics
S01	97.53%	97.37%
S02	91.97%	89.50%
S03	88.32%	89.07%
S04	95.53%	96.06%
S05	90.88%	91.45%
S06	94.15%	93.60%
S07	71.69%	73.34%
S08	86.53%	86.26%
S09	94.56%	94.62%
S10	93.69%	93.84%
<b>W. Avg.</b>	<b>90.73%</b>	<b>90.69%</b>

It is difficult to directly compare the results of this algorithm with existing methods in literature since most algorithms use signals extracted from the chest region for heart sound segmentation. Table 2 shows the performance of several heart sound segmentation algorithms which were discussed in Section 1, their test data size and number of subjects used in the study. In all these cases the sensor for data acquisition was placed on the chest except in this work and [14] where it was placed on the neck.

**Table 2** Comparison of dataset size and results obtained in this algorithm with other works in the literature.

Reference	Test data	Subjects	Results
[3]	515 cycles	37	93% and 84%
[4]	1165 cycles	77	96.7% and 92.9%
[5]	263 cycles	-	79.30%
[2]	7530 cycles	55	97.95%
[6]	207 cycles	-	93.20%
[7]	1600 sec.	80	95%
[8]	2286 sec.	9	98%
[9]	700 cycles	8	99.1% for S2
[14]	80 min.	8	3.4 bpm std dev
[10]	357 cycles	71	97.47
[11]	326 cycles	53	91.47% and 88.95%
[12]	340 cycles	41	90.29%
[13]	-	3	2.4 bpm RMS error
<b>This work</b>	<b>38.4 hours</b>	<b>10</b>	<b>90.70%</b>

Table 3 shows the estimation error bias and standard deviation in beats per minute for each subject with respect to the external Konica-Minolta and SomnoMedics systems. Overall, for most subjects the algorithm gives considerably good bias and standard deviation results for a much larger dataset than that used in [14].

The sensor used for recording signals in this work was originally designed to monitor breathing [15]. It was designed to be comfortable and easy to use. During a pilot clinical study of its use in apnoea detection, all the patients gave it a very high rating on comfort level [19]. The results in this paper show that apart from monitoring the breathing, it is also possible to extract heart rate from the same sensor placed on the same location. This is highly advantageous for wearable health monitors since it obviates the need to use a different sensor to monitor heart rate. In other words, it could reduce the number of sensors required to be placed on a patient thus making it more comfortable for them to use in long term monitoring. However, because the algorithm is specifically designed to work with the heart sounds obtained at the suprasternal notch, it is unlikely to perform well *as is* on sounds obtained from any other location. In that sense, the algorithm is linked to

**Table 3** List of value difference bias and standard deviation (SD) between the algorithm heart rate output and those from Konica-Minolta and SomnoMedics device in beats per minute (bpm) for each subject.

Subject	Konica-Minolta		SomnoMedics	
	Bias (bpm)	SD (bpm)	Bias (bpm)	SD (bpm)
S01	0.15	2.30	0.15	2.30
S02	-0.66	3.11	-0.68	3.15
S03	1.40	7.62	1.40	7.62
S04	0.45	4.62	0.45	4.62
S05	2.04	7.40	2.07	7.60
S06	0.43	5.96	0.43	5.96
S07	6.77	21.42	6.77	21.42
S08	1.57	7.23	1.57	7.23
S09	-0.43	3.26	-0.43	3.26
S10	1.01	6.78	1.01	6.78

the sensor location and will need to be adjusted to work with the traditional heart sounds.

Although the algorithm has been tested on a much larger dataset than any other, the number of subjects is comparatively low since this was only a pilot study to prove the feasibility of this method. Future work involves a greater clinical trial with a higher number of test subjects. Overall, the results in this paper illustrate a strong proof of concept for heart rate monitoring using acoustic signals from the suprasternal notch. This has been demonstrated with the development of a novel heart rate extraction algorithm and its performance evaluation on a large dataset of over 38 hours. The acoustic heart rate algorithm presented in this paper also represents an advance in the field of acoustic heart rate monitoring beyond its conventional use where sensors are placed on the chest. These results will be highly useful for designers and researchers in wearable health monitoring systems by opening up the possibility of using alternative sensor location thereby using a single sensor to monitor multiple vital signs.

## 5 References

- [1] L. A. Geddes, "Birth of the stethoscope," *IEEE Eng Med Biol Mag*, vol. 24, no. 1, pp. 84–6, 2005.
- [2] D. Kumar, P. Carvalho, M. Antunes, P. Gil, J. Henriques, and L. Eugenio, "A new algorithm for detection of S1 and S2 heart sounds," in *IEEE ICASSP*, Toulouse, May 2006.
- [3] H. Liang, S. Lukkarinen, and I. Hartimo, "Heart sound segmentation algorithm based on heart sound envelopegram," in *Computers in Cardiology*, Lund, September 1997.
- [4] H. Y. Liang, L. Sakari, and H. Iiro, "A heart sound segmentation algorithm using wavelet decomposition and reconstruction," in *IEEE EMBC*, Chicago, October 1997.
- [5] M. Brusco and H. Nazeran, "Development of an intelligent pda-based wearable digital phonocardiograph," in *IEEE EMBC*, Shanghai, September 2005.
- [6] P. Wang, Y. Kim, L. H. Ling, and C. B. Soh, "First heart sound detection for phonocardiogram segmentation," in *IEEE EMBC*, Shanghai, September 2005.
- [7] L. G. Gamero and R. Watrous, "Detection of the first and second heart sound using probabilistic models," in *IEEE EMBC*, Cancun, September 2003.
- [8] A. D. Ricke, R. J. Povinelli, and M. T. Johnson, "Automatic segmentation of heart sound signals using hidden markov models," in *Computers in Cardiology*, Lyon, September 2005.
- [9] C. S. Lima and D. Barbosa, "Automatic segmentation of the second cardiac sound by using wavelets and hidden markov models," in *IEEE EMBC*, Vancouver, August 2008.

- [10] S. Ari, P. Kumar, and G. Saha, "A robust heart sound segmentation algorithm for commonly occurring heart valve diseases," *J Med Eng Technol*, vol. 32, no. 6, pp. 456–65, 2008.
- [11] M. Yamacli, Z. Dokur, and T. Ölmez, "Segmentation of S1-S2 sounds in phonocardiogram records using wavelet energies," in *IEEE ISICIS*, Istanbul, October 2008.
- [12] C. N. Gupta, R. Palaniappan, S. Swaminathan, and S. M. Krishnan, "Neural network classification of homomorphic segmented heart sounds," *Applied Soft Computing*, vol. 7, no. 1, pp. 286–297, 2007.
- [13] Y.-H. Chen, H.-H. Chen, T.-C. Chen, and L.-G. Chen, "Robust heart rate measurement with phonocardiogram by on-line template extraction and matching," in *IEEE EMBC*, Boston, September 2011.
- [14] B. Popov, G. Sierra, V. Telfort, R. Agarwal, and V. Lanzo, "Estimation of respiratory rate and heart rate during treadmill tests using acoustic sensor," in *IEEE EMBC*, Shanghai, September 2005.
- [15] P. Corbishley and E. Rodriguez-Villegas, "Breathing detection: Towards a miniaturized, wearable, battery-operated monitoring system," *IEEE Trans. Biomed. Eng.*, vol. 55, no. 1, pp. 196–204, 2008.
- [16] A. M. Weessler, W. S. Harris, and C. D. Schoenfeld, "Systolic time intervals in heart failure in man," *Circulation*, vol. 37, no. 2, pp. 149–59, 1968.
- [17] SOMNOmedics GmbH. (2014) SOMNOscreen. [Online]. Available: <http://www.somnomedics.eu/>.
- [18] Konica Minolta. (2014) Oxygen Saturation Monitor PULSOX-300i. [Online]. Available: <http://www.konicaminolta.com/>.
- [19] E. Rodriguez-Villegas, G. Chen, J. Radcliffe, and J. Duncan, "A pilot study of a wearable apnoea detection device," *BMJ Open*, vol. 4, no. 10, 2014.